Exposure to 5G mmWaves of a Base Station Operator: Dosimetric Study of the Influence of Posture

Luca Bellosono[#*], Simona D'Agostino[#], Micol Colella[#], Gian Marco Contessa[*], Alessandro Polichetti[*], Micaela Liberti[#], Francesca Apollonio[#]

[#]Dept. of Information Engineering, Electronics and Telecommunications, Sapienza University of Rome, Italy

[*]National Center for Radiation Protection and Computational Physics, Italian National Institute of Health, Italy,

{luca.bellosono, simona.dagostino, micol.colella, micaela.liberti, francesca.apollonio}@uniroma1.it,
{gianmarco.contessa, alessandro.polichetti}@iss.it

2024 International Symposium on Electromagnetic Compatibility – EMC Europe | 979-8-3503-0735-1/24/$31.00 ©2024 IEEE | DOI: 10.1109/EMCEurope59828.2024.10722266

***Abstract* — In this work, the electric field induced by plane wave exposure inside a human model is numerically investigated. The focus has been on workers exposed to electromagnetic fields at the frequency of 26 GHz, belonging to the FR2 band of 5G technology. The results were obtained adopting a human anatomical model, studying an exposure scenario corresponding to the reference levels for local occupational exposure. The analysis was conducted on a specific anatomical region, i.e., the wrist, in different positions of the arm. The results show how the induced electric field may depend on the posture of the exposed subject and their anatomical characteristics.**

***Keywords* — 5G, Millimiter-wave, Electromagnetic fields, Occupational exposure, Plane wave.**

I. Introduction

In recent years, the increase of technologies related to 5G has risen concerns about exposure to electromagnetic fields (EM) fields. Despite international guidelines, such as those outlined by the International Commission on Non-Ionizing Radiation Protection (ICNIRP) [1], [2], as well as the establishment of minimum safety provisions related to workers' exposure [3], the assessment of risk for workers remains a topic of discussion [4], [5], [6].

In this context, computational studies play a fundamental role as they allow for the investigation of dosimetric quantities induced by external EM fields within the human body, which is inaccessible through experimental approaches [7], [8], [9]. For studying induced quantities in the human body at 5G frequencies, the Finite-Difference Time-Domain (FDTD) method can be used. This method is advantageous for such type of studies because it allows modelling complex geometries, taking into account their shapes, thereby obtaining an excellent representation of the anatomy of biological tissues in the human body.

While for frequencies below 6 GHz, the application of the FDTD method to solve Maxwell's equations within the human body can be adopted requiring accessible computational load, at higher frequencies, the increase in computational cost has led to the use of simplified 1-D anatomical models [10], [11].

This choice is justified by the fact that for frequencies within the mmWave band (specifically close to 30 GHz), the penetration depth of the EM field decreases, making the skin the tissue of greatest interest for dosimetric studies. Such simplified approaches, however, do not consider the anatomical shape of the body and, as demonstrated in [12], [13] the use of slabs compared to the realistic 3-D model leads to significant differences in the results obtained (up to 2 dB).

Considering the rapid proliferation of technologies such as Multiple Input Multiple Output (MIMO) antennas in telecommunications [14], [15], [16], starting from the results obtained in [13], we analyse a scenario where a base station maintenance worker is exposed to a plane wave at the frequency of 26 GHz, which is in the Frequency Range 2 (FR2) of the 5G radio access of mobile networks. The study focuses on a specific anatomical region, the wrist since it is characterized by a prominent curvature [13].

The exposure scenario evaluated herein was set to ensure compliance with reference levels at 26 GHz for local occupational exposures longer than 6 minutes as suggested by ICNIRP in 2020 [2].The induced electric field in the worker's wrist was evaluated in three different positions showing the role of the posture of the subject and of the anatomical characteristics in the outcomes of this exposure assessment in the deeper layers of the body.

II. Materials and Methods

A. Exposure Conditions

In Fig. 1a an example of a possible posture adopted by base station workers is shown. Based on a dedicated analysis on typical operational conditions for base station workers, it emerged that typically, maintenance work is carried out on the electronic apparatus located beneath the radiobase site. For this reason and considering the posture in Fig. 1a, we evaluated far field exposure of the wrist, in three different tilting positions. The 3-D anatomical model used for this study is the Virtual Population human male model Duke (ViP, v. 3.1) [17]. This model is representative of a 34-year-old man, 1.77 m tall and 77 kg of weight. It counts more than 300 body structures, among which are a homogeneous layer of epidermis and dermis, subcutaneous fat and muscle. Once the Duke model was imported, the Poser tool was used to place the right arm in the same horizontal position studied in [13] (reference position) and in two additional arm positions.

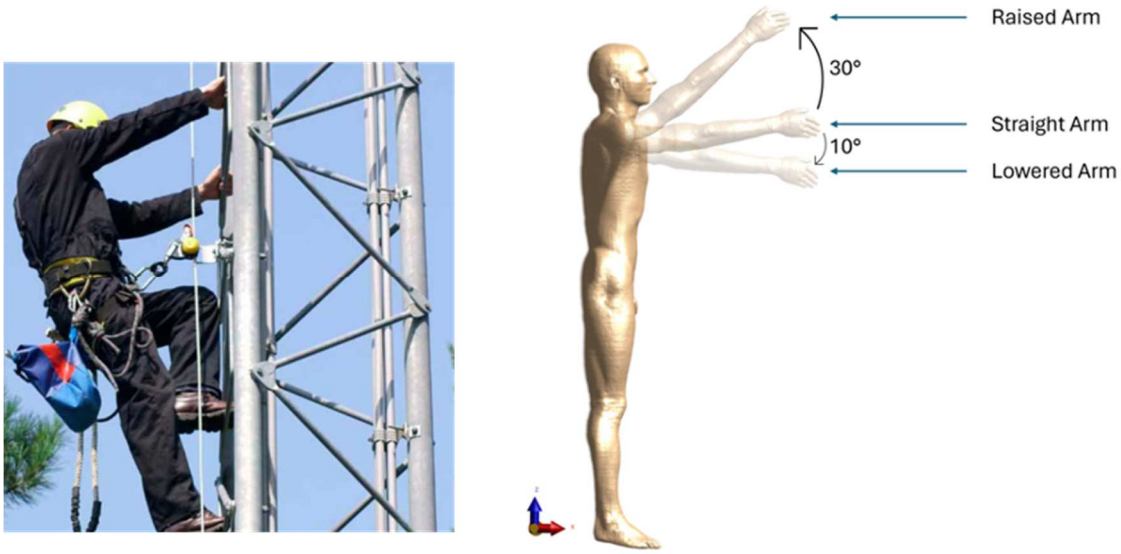

Fig. 1. a) Example of a possible posture adopted by a maintenance worker operating on a base station. b) the 3-D Model Duke with the right arm positioned in the three cases of interest: straight arm, raised arm and lowered arm. (lateral view).

Consequently, three different simulations were performed: one with the arm in the reference position, another with the arm raised by +30° relative to the reference position, and a third with the arm lowered by -10° relative to the reference position (Fig. 1b). Here, these three positions were respectively named "straight arm," "raised arm," and "lowered arm," representing the three cases analyzed for this study. Far field exposure is simulated by a plane wave as in [13].

As exposure domain within which the plane wave propagates, a space with dimensions of 606×246×514 mm^3 was simulated to contain only the arm of the anatomical model (Fig. 2, red wireblock). As a region of interest for the exposure, the area of the wrist (80×87×30 mm^3) was selected (Fig. 2, black wireblock).

The domain, as well as the region of interest, are the same for the three simulations and are adapted from the conditions assessed in previous studies [12], [13], [19], [20].

The wrist is exposed to an incident plane wave at 26 GHz, propagating perpendicularly to the z-axis (Fig. 2). This polarization is characterized by the triple E-H-k shown in Fig. 2, where E and H are the electric and magnetic field vectors, respectively, and k is the wave vector. Thus, the plane wave incidence is perpendicular in the “straight arm” scenario, while it occurs at different angles in the “raised arm” and “lowered arm” scenarios. This plane wave impinges with an incident power density of 154.5 W/m^2 (rms), which corresponds to the ICNIRP 2020 reference level for local occupational exposures longer than 6 minutes at 26 GHz [2].

B. Simulation Setup

Three different simulations were performed, one for each scenario of analysis: “straight arm”, “raised arm”, and “lowered arm”. The FDTD method was implemented in the simulation software Sim4Life (v. 7.2, Zurich Medtech, AG). The EM properties of each tissue were assigned from the IT’IS database [18] at the frequency of interest and a non-uniform grid was applied in all the three scenarios, with a minimum step of 0.1 mm in the anatomical area of interest and a maximum of 0.87 mm in the rest of the domain, resulting in 1.3 GCells, 1.9 GCells, and 1.5 GCells for the “straight arm”, “raised arm” and “lowered arm”, respectively.

Absorbing boundary conditions were set using ten layers of perfectly matched layer (PML) material, and 20 cells of free space were added around the voxel domain.

III. Results

The results on the E-field induced in the three exposure conditions are shown in Fig. 3 on a transversal plane crossing the center of the wrist. The distributions of the E-field, expressed in dB, in a slice of the wrist for the three cases of interest can be observed. As expected for all three positions of the arm, the maximum values of E-field occur around the superficial skin.

To further evaluate the differences between the three exposure conditions, we focused on a region of interest (ROI) with a width of 15 mm and a depth of 4 mm (Fig. 3, black squares). The trend of the E-field along a reference line here called “Central Line”, at the center of the ROI was evaluated. In Fig. 4, the trend of E-field for the three cases of interest within the ROI can be observed. Comparing the behaviour of E-field (dB) with increasing depth for the three cases (Fig. 4), it is evident that the trends are very similar, with the maximum values occurring at the air-skin interface.

The “Raised Arm” curve is placed between the “Straight Arm” and “Lowered Arm” curves, with a maximum spread close to 2 dB. Table 1 reports the induced E-field values at the interface and at different depths up to 4 mm. Despite the high value of E at the air-skin interface, exceeding 100 V/m for all three cases (117.54 V/m, 105.43 V/m, 101.54 V/m respectively for “straight arm”, “raised arm”, and “lowered arm”), the intensity of the field decreases by approximately

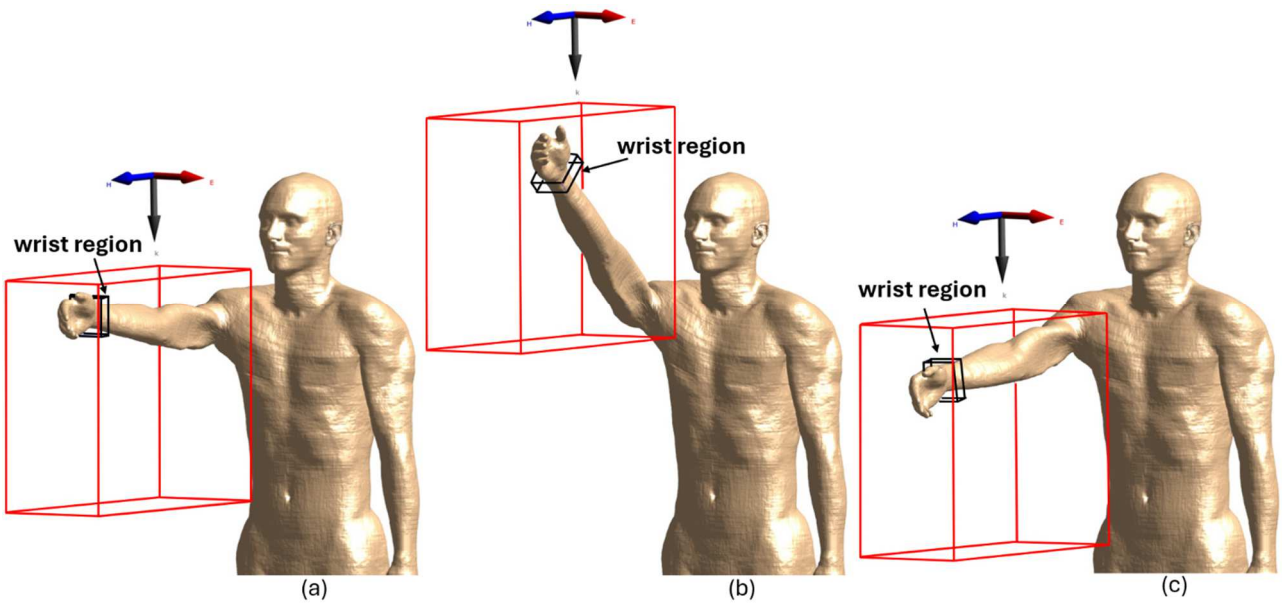

Fig. 2. Investigated exposure scenarios and plane wave propagation direction: (a) straight arm, (b) raised arm, (c) lowered arm.

60% after only 1 mm of depth and loses about 90% of its intensity after 3 mm.

The differences in the calculated values in the three cases of interest (Table 1) can be attributed to the varying angle of incidence of the plane wave on the wrist, determined by the different positions of the arm.

For all the depths considered, the E-field values of "Straight Arm" position are always the highest, while the E-field values of "Lowered Arm" are always the lowest. At z=1mm the difference in results between the "Straight Arm" (reference) and "Raised Arm" positions is greater to 10%, which is comparable to what has been obtained in [13] where the anatomical scenario has been compared to the 1D planar layer.

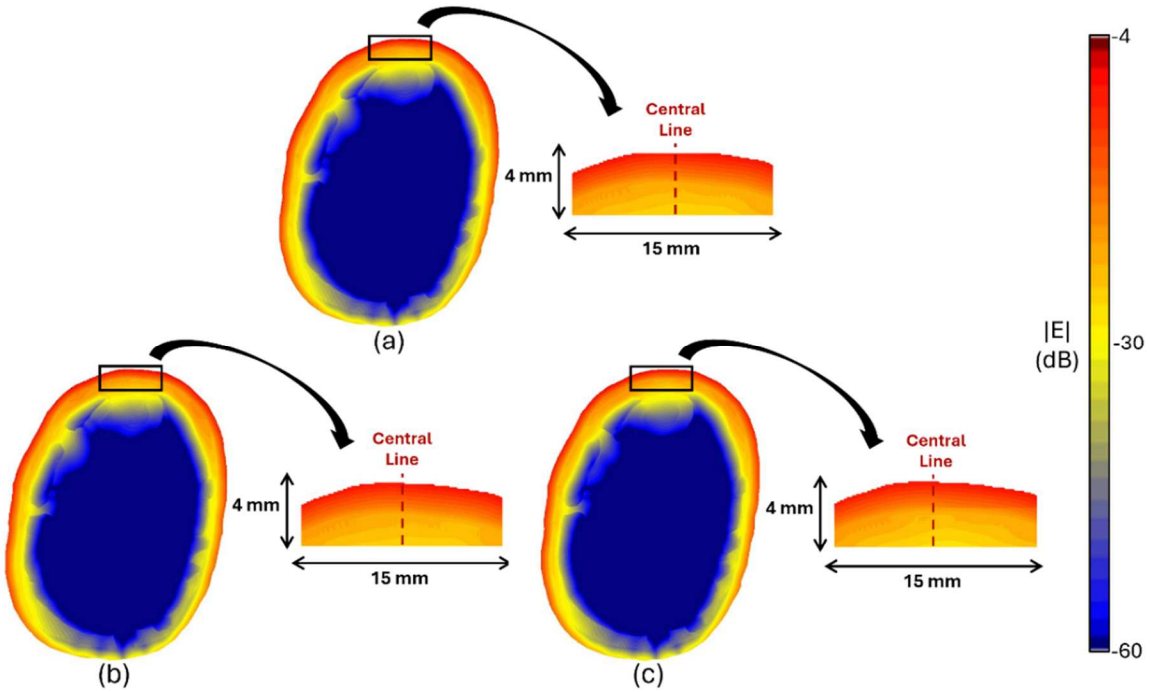

Fig. 3. Details of the E-field in the region of the wrist and in the ROI down to 4 mm inside the tissues; incident E-field (341 V/m, peak). Left: E-field distribution in the tissues and in the black square the region of interest (ROI). Right: ROI. The red dotted line identifies the "Central Line" along which the E-field were calculated. (a) straight arm, (b) raised arm, (c) lowered arm.

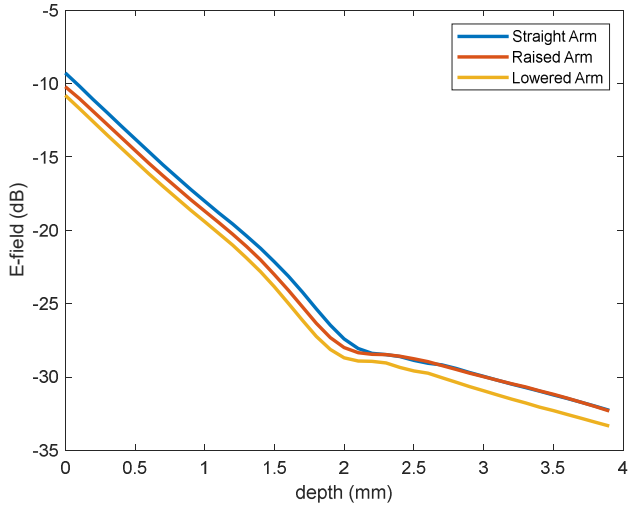

Fig. 4. Comparison between the E-field trend along the "Central Line" for the 3 cases of interest.

Table 1. Induced E-field value at the interface and at the various depths inside the skin.

	$E_{interface}$ (V/m)	$E_{z=1mm}$ (V/m)	$E_{z=2mm}$ (V/m)	$E_{z=3mm}$ (V/m)	$E_{z=4mm}$ (V/m)
Straight Arm	117.15	42.90	14.56	10.84	8.32
Raised Arm	105.43	39.68	13.58	10.82	8,28
Lowered Arm	101.54	36.51	12.55	9.68	7.34

IV. Discussion and Conclusions

The aim of this work was to investigate whether the position of the arm influences the induced electric field due to different plane wave incident direction. To carry out such analysis we considered a particular scenario with a base station worker exposed to a plane wave impinging on the surface of the arm at 26 GHz. Starting from previous studies [12], [13], [19], [20], which evaluated the local exposure of three different body parts (i.e., back, arm and wrist) to an impinging plane wave, we reproduced a similar scenario focusing on the wrist. For this anatomical district three different tilting angles of the arm were considered, which are intended to simulate a worker performing maintenance on the electronic apparatus located beneath the radiobase site, allowing to consider a far-field exposure. The exposure was set to guarantee a safety condition, which implies to consider an incident power density equal to 154.5 W/m^2 that ensures compliance with reference levels at 26 GHz for local occupational exposures longer than 6 minutes as suggested by ICNIRP in 2020 [2]. This assumption was intended to put us in an initial condition where the limits were already respected. Therefore, no further verification was carried out. The dosimetric study of the induced electric field, on the contrary, serves primarily to carry out a comparison with both the reference paper [13] and the new positions herein analyzed in the deeper layers of the body.

The results obtained show that the highest electric field values are localized in the superficial part of the skin. As expected for such high frequencies, the electric field magnitude decreases rapidly as it penetrates the biological tissue. After just 1 mm of depth, the intensity calculated in the wrist decreases by approximately 60%, and after 3 mm, by 90%. Furthermore, the differences in the calculated values for the induced electric field in the three exposure scenarios may depend on the posture of the exposed subject relative to the angle of incidence of the plane wave.

The analysis carried out in this study allowed us to take into account the effect of the body shape [12], [13], [19], [20] by considering exposure of an anthropomorphic human body model. As a drawback, the stratification of the skin is neglected.

Future evaluations will be carried out to account for a more detailed stratification of the skin, as well as the exposure assessment related to other part of the body, that may be more of interest in term of safety and from the protectionism point of view. Additionally, a more in-depth study concerning other dosimetric quantities (e.g. absorbed power density) will be analyzed and studied in future works.

References

[1] R. Matthes, J. H. Bernhardt, A. F. McKinlay, and International Commission on Non-Ionizing Radiation Protection., Guidelines on limiting exposure to non-ionizing radiation : a reference book based on the guidelines on limiting exposure to non-ionizing radiation and statements on special applications. International Commission on Non-Ionizing Radiation Protection, 1999.

[2] G. Ziegelberger et al., "Guidelines for limiting exposure to electromagnetic fields (100 kHz to 300 GHz)," Health Physics, vol. 118, no. 5. Lippincott Williams and Wilkins, pp. 483–524, May 01, 2020. doi: 10.1097/HP.0000000000001210.

[3] "I (Legislative acts) DIRECTIVE 2013/35/EU OF THE EUROPEAN PARLIAMENT AND OF THE COUNCIL of 26 June 2013 on the minimum health and safety requirements regarding the exposure of workers to the risks arising from physical agents (electromagnetic fields) (20th individual Directive within the meaning of Article 16(1) of Directive 89/391/EEC) and repealing Directive 2004/40/EC."

[4] R. Stam, "Occupational exposure to radiofrequency electromagnetic fields," Industrial Health, vol. 60, no. 3. National Institute of Industrial Health, pp. 201–215, 2022. doi: 10.2486/indhealth.2021-0129.

[5] A. Modenese and F. Gobba, "Occupational exposure to electromagnetic fields and health surveillance according to the european directive 2013/35/eu," Int J Environ Res Public Health, vol. 18, no. 4, pp. 1–12, Feb. 2021, doi: 10.3390/ijerph18041730.

[6] K. Karipidis, R. Mate, D. Urban, R. Tinker, and A. Wood, "5G mobile networks and health—a state-of-the-science review of the research into low-level RF fields above 6 GHz," Journal of Exposure Science and Environmental Epidemiology, vol. 31, no. 4. Springer Nature, pp. 585–605, Jul. 01, 2021. doi: 10.1038/s41370-021-00297-6.

[7] A. Hirata et al., "Human exposure to radiofrequency energy above 6 GHz: Review of computational dosimetry studies," Physics in Medicine and Biology, vol. 66, no. 8. IOP Publishing Ltd, Apr. 21, 2021. doi: 10.1088/1361-6560/abf1b7.

[8] S. D'Agostino, M. Colella, M. Liberti, R. Falsaperla, and F. Apollonio, "Systematic numerical assessment of occupational exposure to electromagnetic fields of transcranial magnetic stimulation," Med Phys, vol. 49, no. 5, pp. 3416–3431, May 2022, doi: 10.1002/mp.15567.

[9] M. Colella et al., "Numerical Evaluation of Human Body Near Field Exposure to a Vehicular Antenna for Military Applications," Front Public Health, vol. 9, Feb. 2022, doi: 10.3389/fpubh.2021.794564.

[10] G. Sacco, S. Pisa, and M. Zhadobov, "Age-dependence of electromagnetic power and heat deposition in near-surface tissues in

emerging 5G bands," Sci Rep, vol. 11, no. 1, Dec. 2021, doi: 10.1038/s41598-021-82458-z.

[11] M. C. Ziskin, S. I. Alekseev, K. R. Foster, and Q. Balzano, "Tissue models for RF exposure evaluation at frequencies above 6 GHz," Bioelectromagnetics, vol. 39, no. 3. Wiley-Liss Inc., pp. 173–189, Apr. 01, 2018. doi: 10.1002/bem.22110.

[12] M. Colella, S. Di Meo, M. Liberti, M. Pasian, and F. Apollonio, "Numerical comparison of plane wave propagation inside realistic anatomical models and multilayer slabs," in 2022 52nd European Microwave Conference (EuMC), 2022, pp. 800–803. doi: 10.23919/EuMC54642.2022.9924362.

[13] M. Colella, S. Di Meo, M. Liberti, M. Pasian, and F. Apollonio, "Advantages and Disadvantages of Computational Dosimetry Strategies in the Low mmW Range: Comparison between Multilayer Slab and Anthropomorphic Models," IEEE Trans Microw Theory Tech, vol. 71, no. 10, pp. 4533–4545, Oct. 2023, doi: 10.1109/TMTT.2023.3267568.

[14] S. Q. Wali, A. Sali, J. K. Allami, and A. F. Osman, "RF-EMF Exposure Measurement for 5G Over Mm-Wave Base Station With MIMO Antenna," IEEE Access, vol. 10, pp. 9048–9058, 2022, doi: 10.1109/ACCESS.2022.3143805.

[15] X. Gao, O. Edfors, F. Rusek, and F. Tufvesson, "Massive MIMO Performance Evaluation Based on Measured Propagation Data," IEEE Trans Wirel Commun, vol. 14, no. 7, pp. 3899–3911, Jul. 2015, doi: 10.1109/TWC.2015.2414413.

[16] IEEE Communications Society and Institute of Electrical and Electronics Engineers, 2017 IEEE Global Communications Conference (GLOBECOM) : proceedings : Singapore, 4-8 December 2017.

[17] M. C. Gosselin et al., "Development of a new generation of high-resolution anatomical models for medical device evaluation: The Virtual Population 3.0," Phys Med Biol, vol. 59, no. 18, pp. 5287–5303, Sep. 2014, doi: 10.1088/0031-9155/59/18/5287.

[18] "P. A. Hasgall et al., 'IT'IS database for thermal and electromagnetic parameters of biological tissues, version 4.1,' Feb. 2022, doi: 10.13099/VIP21000-04-1."

[19] M. Colella, S. Di Meo, M. Pasian, M. Liberti, and F. Apollonio, "Effect of Realistic Body Models on Plane Wave Reflection at mmWaves," in 2023 IEEE MTT-S International Microwave Biomedical Conference, IMBioC 2023, Institute of Electrical and Electronics Engineers Inc., 2023, pp. 142–144. doi: 10.1109/IMBioC56839.2023.10305090.

[20] European Microwave Association, 2021 51st European Microwave Conference 4-6 April 2022, London, UK.